Cooperative control of autonomous tugs for ship towing

Du, Zhe; Reppa, Vasso; Negenborn, Rudy R.

DOI
10.1016/j.ifacol.2020.12.1448

Publication date
2020

Document Version
Final published version

Published in
IFAC-PapersOnline

Available online at www.sciencedirect.com

ScienceDirect

IFAC PapersOnline CONFERENCE PAPER ARCHIVE

IFAC PapersOnLine 53-2 (2020) 14470–14475

Cooperative Control of Autonomous Tugs for Ship Towing

Zhe Du, Vasso Reppa, Rudy R. Negenborn

Department of Maritime and Transport Technology, Delft University of Technology, Delft, The Netherlands (e-mail: Z.Du@tudelft.nl).

Abstract: Autonomous surface vehicles (ASVs) are seeing a significant development over the last decade. In recent years, their commercial applications are attracting the attention of many companies. One of the promising subjects is to develop autonomous tugs for ship berthing. This paper focuses on the cooperative control of autonomous tugs for ship towing in a berthing scenario. We propose a multi-layer optimal control strategy for a two-tug towing system to guarantee a ship reaching a desired position with a desired heading and velocity. In the higher layer supervisory control, an optimal control method is used to allocate towing forces and determine towing angles. With the help of these results and geometry relationships, the reference trajectories of the two autonomous tugs can be calculated online. Based on the reference trajectories, the trajectory tracking, which is in the lower layer, is addressed. Simulation results indicate that two autonomous tugs can cooperatively tow the unpowered ship to a desired position with a desired heading and velocity.

Keywords: Cooperative control, Autonomous surface vehicles, Multi-vessel systems, Multi-layer optimal control, Ship manipulation

1. INTRODUCTION

Unmanned surface vehicles (USVs) have been developed since the 1940s, but most of them are remotely controlled vessels(Portmann et al. (2002)). Only during the last decade have we seen significant development of autonomous surface vehicles (ASVs). Their applications include early military deployment (Roberts and Sutton (2006)), latter scientific research (Bertram (2008); Manley (2008)) and now commercial uses (Liu et al. (2016); Yan et al. (2010)). Starting in 2017, some marine related companies have already launched future projects to develop the commercial autonomous vessels (Devaraju et al. (2018)). According to their plans, tugs will be one of the first vessel classes to become autonomous and the first step to unmanned autonomous shipping. As such, autonomous tugs will be a promising research area for emerging commercial applications.

The working process of autonomous tugs involves an object manipulation problem applied on the water. According to the way of connection, solutions can be classified into two categories. The first one is the fixed attachment. Scholars (Bidikli et al. (2016); Bui et al. (2012); Esposito et al. (2008); Sartoretti et al. (2016); Smith et al. (2007)) take advantage of a swarm of ASVs to attach in a fixed way to a large ship or floating platform. These ASVs are treated as actuators to offer the power for moving the object. The object manipulation problem is then transformed to the control allocation problem (Johansen and Fossen (2013)). Since this way of object manipulation is a common practice in robotics, control methods used in robotics can then be directly applied here. However, when considering the congested navigation environment and bad weather conditions, this way is not safe for the manipulated object. On the one hand, the ASV attachment increases the scale of the object, which may lead to a collision with other vessels in the restricted waterways. On the other hand, the weather disturbances make the motion of the ASV and the object asynchronous, which may cause the attachment to break.

Considering the common practice of marine operations and the performance of tugs (Hensen (2003)), the "soft" connection is an alternative to the fixed approach to deal with object manipulation on the water. The object is transported by ropes or cables connected to multiple tugs. The manipulation ways are categorized as caging and towing. Caging manipulation is suitable for liquid floating objects, the typical application is oil skimming (Bhattacharya et al. (2011); Giron-Sierra et al. (2014); Pereda et al. (2011)). The spilled oil is captured and transported by a boom (the device that can prevent oil from floating around) through controlling the motion of two ASVs. Towing manipulation is suitable for a large solid object, with typical application marine floating facility transportation. In some research works (Hajieghrary et al. (2017); Yun and Jian (2018)), the authors take advantage of a soft connection with cables to control the manipulated unpowered facility tracking a predefined trajectory. However, for most of the application scenarios like assisted ship berthing, while guaranteeing the safety of the ship, not only the position but also the heading and velocity should be controlled.

Therefore, to fill the gap of the above literatures, we propose a multi-layer optimal control strategy for ship towing to manipulate the ship reaching a desired position with desired heading and velocity. The higher-layer control al-

10.1016/j.ifacol.2020.12.1448

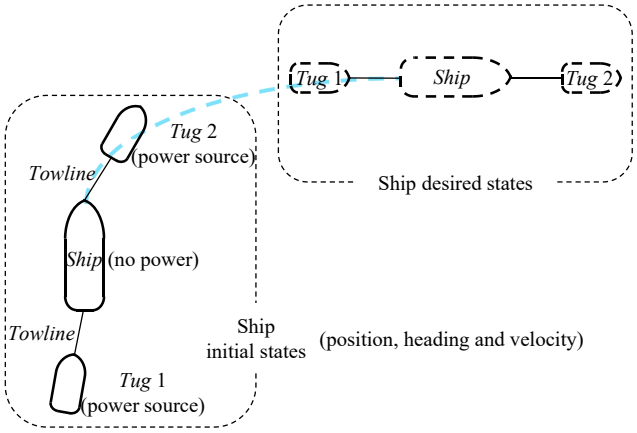

Fig. 1. Towing system and the control objective.

locates the towing forces and determines the towing angles based on the desired states of the ship. According to the results, the reference trajectories of the two autonomous tugs can be calculated online, and the lower-layer control tracks these two online trajectories.

The paper is organized as follows: Section 2 describes the main problem and transfers it into a mathematical model. The design of the multi-layer control approach is given in Section 3. In Section 4, simulation experiments are carried out to illustrate the potential of the proposed method. Conclusions and future research directions are given in Section 5.

2. PROBLEM STATEMENT

Consider a towing system that consists of one ship and two tugs as shown in Fig. 1. The forward Tug 2 and aft Tug 1 are connected to the Ship by a towline. In the berthing scenario the ship is assumed to have no power, so the power sources (control inputs) of the system come from the two tugs. The control objective is to move the ship from the initial states (position, heading and velocity) to the desired states.

Assuming no environmental disturbances, a simplified 3-DOF (degree of freedom) vessel model is considered in this paper. The kinematics and kinetics can be expressed as (Fossen (2011)):

$$\begin{aligned} &\dot{\boldsymbol{\eta}}(t) = \boldsymbol{R}(\psi(t))\boldsymbol{\nu}(t) \\ &\boldsymbol{M}\dot{\boldsymbol{\nu}}(t) + \boldsymbol{C}(\boldsymbol{\nu}(t))\boldsymbol{\nu}(t) + \boldsymbol{D}\boldsymbol{\nu}(t) = \boldsymbol{\tau}(t), \end{aligned} \tag{1}$$

where $\boldsymbol{\eta}(t)=[x(t)\ \ y(t)\ \ \psi(t)]^{\mathrm{T}}\in\mathbb{R}^3$ is the position vector in the world frame (North-East-Down) including ship position coordinates ($x(t)$, $y(t)$) and heading $\psi(t)$; $\boldsymbol{\nu}(t)=[u(t)\ \ v(t)\ \ r(t)]^{\mathrm{T}}\in\mathbb{R}^3$ is the velocity vector in the Body-fixed frame containing the velocity of surge $u(t)$, sway $v(t)$ and yaw $r(t)$; $\boldsymbol{R}\in\mathbb{R}^{3\times3}$ is the rotation matrix from the body frame to the world frame, which is a function of heading; $\boldsymbol{M}\in\mathbb{R}^{3\times3}$, $\boldsymbol{C}\in\mathbb{R}^{3\times3}$ and $\boldsymbol{D}\in\mathbb{R}^{3\times3}$ are the Mass (inertia), Coriolis-Centripetal and Damping matrix, respectively; $\boldsymbol{\tau}(t)=[\tau_u(t)\ \ \tau_v(t)\ \ \tau_r(t)]^{\mathrm{T}}\in\mathbb{R}^3$ is the controllable input referring to the forces $\tau_u(t)$, $\tau_v(t)$ and moment $\tau_r(t)$ offered by actuators in the Body-fixed frame.

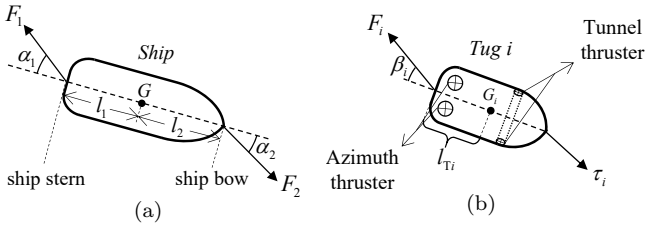

Fig. 2. Schematic diagram of the physical system: (a) Ship; (b) Tug.

2.1 Dynamics of the Ship

In this work, we assume that the ship cannot move by itself. The power that move the ship is the forces from the towlines applied by the two tugs (as shown in Fig. 2 (a)), which can be expressed as:

$$\boldsymbol{\tau}(t) = -\boldsymbol{B}(\alpha_1(t))F_1(t) + \boldsymbol{B}(\alpha_2(t))F_2(t), \tag{2}$$

where $F_1(t)$ and $F_2(t)$ are the towing forces of the aft (Tug 1) and forward (Tug 2), respectively. We assume there is no force loss on the towline. $\boldsymbol{B}$ is the configuration matrix which is a function of the towing angle ($\alpha_i(t)$), expressed as:

$$\boldsymbol{B} = \begin{bmatrix} \cos(\alpha_i(t)) \\ \sin(\alpha_i(t)) \\ l_i\sin(\alpha_i(t)) \end{bmatrix} \quad (i=1,2), \tag{3}$$

where l_i is the distance from the center of gravity of the ship (G) to the ship stern (l_1) or the ship bow (l_2).

2.2 Dynamics of the Tugs

In order to meet the flexibility in ship berthing assisting, the actuator system of the tug generally contains two stern azimuth thrusters and one bow tunnel thruster, known as the *ASD tug* (Hensen (2003)). With the help of three thrusters, the tug can obtain omnidirectional forces and moments. So the control inputs of the tugs consist of the reaction towing force and the thrusters (as shown in Fig. 2 (b)). The kinetics of the tugs can be expressed as:

$$\begin{aligned} &\boldsymbol{M_i}\dot{\boldsymbol{\nu}}_{\boldsymbol{i}}(t) + \boldsymbol{C_i}(\boldsymbol{\nu_i}(t))\boldsymbol{\nu_i}(t) + \boldsymbol{D_i}\boldsymbol{\nu_i}(t) \\ &= \boldsymbol{\tau_{F_i}}(t) + \boldsymbol{\tau_i}(t) \quad (i=1,2), \end{aligned} \tag{4}$$

where $\boldsymbol{\tau_i}(t)=[\tau_{u_i}(t)\ \ \tau_{v_i}(t)\ \ \tau_{r_i}(t)]^{\mathrm{T}}\in\mathbb{R}^3$ is the forces $\tau_{u_i}(t)$, $\tau_{v_i}(t)$ and moment $\tau_{r_i}(t)$ offered by tug thrusters; $\boldsymbol{\tau_{F_i}}(t)\in\mathbb{R}^3$ is the reaction towing force, expressed as:

$$\begin{aligned} &\boldsymbol{\tau_{F_i}}(t) = \boldsymbol{B_i}(\beta_i(t))F_i(t) \\ &\boldsymbol{B_i} = \begin{bmatrix} \cos(\beta_i(t)) \\ \sin(\beta_i(t)) \\ l_{\mathrm{T}_i}\sin(\beta_i(t)) \end{bmatrix} \quad (i=1,2), \end{aligned} \tag{5}$$

where $\boldsymbol{B_i}$ is the configuration matrix of the tugs; $\beta_i(t)$ is the tugging angle; l_{T_i} is the distance from the center of gravity of the tug (G_i) to the tug stern (l_{T_2}) or the tug bow (l_{T_1}).

Based on the above modelling, it can be seen that the link between the ship system and the tug system is the towing force $F_i(t)$. For the ship, the towing force provides power to move. The effect of $F_1(t)$ is to increase the ship speed

and alter the heading, the effect of $F_2(t)$ is to decrease the ship speed and stabilize the course. For the tugs, the towing force is an external effect which needs to be compensated. Thus, the function of the tug thruster forces and moment $\boldsymbol{\tau_i}(t)$ can be separated into two parts: one is to offer the power to tow the ship (compensate the towing force), another is to offer the power to move the tug itself.

3. MULTI-LAYER CONTROL ARCHITECTURE

According to the characteristics of the towing system and the control objective, a multi-layer control architecture is used (Zheng et al. (2017); Chen et al. (2018)). The towing system is divided into a physical layer and a control layer. The physical layer contains all the hardware equipment, including hull, actuators (thrusters), towlines, computers, sensors, etc. The control layer refers to the software, including the controller and computation unit.

The goal of the controller is to manipulate the ship to a desired place with desired heading and velocity, i.e. $\boldsymbol{\eta} = \boldsymbol{\eta}_{\mathrm{d}}, \boldsymbol{\nu} = \boldsymbol{\nu}_{\mathrm{d}}$. Based on the dynamics equations of the ship and tugs ((1)∼(5)), the control layer is designed as a two-layer structure (shown in Fig. 3).

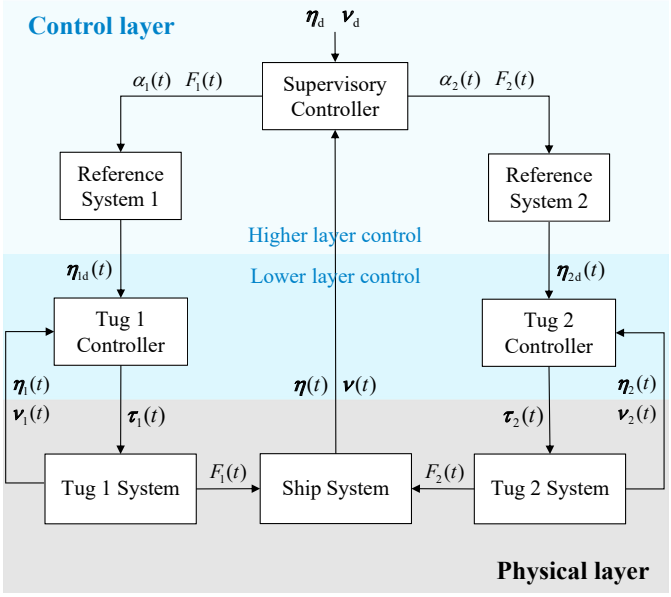

Fig. 3. System control diagram.

In the higher-layer, the goal $(\boldsymbol{\eta}_{\mathrm{d}}, \boldsymbol{\nu}_{\mathrm{d}})$ and measured $(\boldsymbol{\eta}(t), \boldsymbol{\nu}(t))$ ship states are used by the supervisory controller to output the desired towing angles (α_i) and forces (F_i). Then, these results are deployed by the reference system to calculate the desired trajectory $(\boldsymbol{\eta}_{i\mathrm{d}})$ for each tug. In the lower-layer, based on the calculated tug reference trajectories, the two tug controllers input proper forces and moment $(\boldsymbol{\tau}_i)$ into the tug systems to compensate the desired towing forces and move the tugs.

The details of the two control approaches and the reference computation process in the higher-layer are given below.

3.1 Supervisory Controller

The objective of the supervisory controller is to determine the towing forces $(F_i(t))$ and angles $(\alpha_i(t))$ that make the ship reach the desired states $(\boldsymbol{\eta}_{\mathrm{d}}, \boldsymbol{\nu}_{\mathrm{d}})$, given that all the constraints of the ship (plant) and the towing forces and angles (control input) are satisfied, in an optimal way.

The cost function of the supervisory controller is defined as:

$$\begin{aligned} J(t) &= w_1 \boldsymbol{e}_{\boldsymbol{\eta}}^{\mathrm{T}}(t)\boldsymbol{e}_{\boldsymbol{\eta}}(t) + w_2 \boldsymbol{e}_{\boldsymbol{\nu}}^{\mathrm{T}}(t)\boldsymbol{e}_{\boldsymbol{\nu}}(t) \\ \boldsymbol{e}_{\boldsymbol{\eta}}(t) &= \boldsymbol{\eta}_{\mathbf{C}}(t) - \boldsymbol{\eta}_{\mathrm{d}} \\ \boldsymbol{e}_{\boldsymbol{\nu}}(t) &= \boldsymbol{\nu}_{\mathbf{C}}(t) - \boldsymbol{\nu}_{\mathrm{d}}, \end{aligned} \tag{6}$$

where $\boldsymbol{e}_{\boldsymbol{\eta}}(t)\in\mathbb{R}^3$ and $\boldsymbol{e}_{\boldsymbol{\nu}}(t)\in\mathbb{R}^3$ are the position and velocity error, respectively; w_1 and w_2 are the weight coefficients and they are constant and positive scalars; $\boldsymbol{\eta}_{\mathbf{C}}(t)\in\mathbb{R}^3$ and $\boldsymbol{\nu}_{\mathbf{C}}(t)\in\mathbb{R}^3$ are the calculated ship position and velocity, respectively. The calculated ship states satisfy the ship dynamics constraints ((1)∼(3)):

$$\begin{aligned} \dot{\boldsymbol{\eta}}_{\mathbf{C}}(t) &= \boldsymbol{R}(\psi_{\mathrm{C}}(t))\boldsymbol{\nu}_{\mathbf{C}}(t) \\ \dot{\boldsymbol{\nu}}_{\mathbf{C}}(t) &= \boldsymbol{M}^{-1}[-\boldsymbol{C}(\boldsymbol{\nu}_{\mathbf{C}}(t))\boldsymbol{\nu}_{\mathbf{C}}(t) - \boldsymbol{D}\boldsymbol{\nu}_{\mathbf{C}}(t) - \\ &\quad \boldsymbol{B}(\alpha_1(t))F_1(t) + \boldsymbol{B}(\alpha_2(t))F_2(t)], \end{aligned} \tag{7}$$

Apart from the dynamics constraints, according to the physical law and tug practical operation (Hensen (2003)), the towing forces and angles have to satisfy saturation constraints:

$$\begin{aligned} &\alpha_i \in [-\pi/2\ ,\ \pi/2] \\ &F_i \in [0\ ,\ F_{i\max}] \qquad (i = 1, 2), \end{aligned} \tag{8}$$

where $F_{i\max}$ is the maximum value of towing force that the two towlines withstand.

Furthermore, the performance of the trajectory tracking in the lower-layer is related to the quality of the tug reference trajectory, which is affected by the change rate of the towing angles and forces. Thus, a saturation constraint of the change rate for the two towing angles and forces is set to make the reference trajectory smooth:

$$\begin{aligned} &|\dot{\alpha}_i| \le \bar{\alpha}_i \\ &\left|\dot{F}_i\right| \le \bar{F}_i \quad (i = 1, 2), \end{aligned} \tag{9}$$

where $\bar{\alpha}_i$ and $\bar{F}_i$ are the maximum change rate value of towing angle and force, respectively.

3.2 Reference determination

The objective of Reference System in the system control diagram (Fig. 3) is to calculate the expected trajectories, which form a reference for the lower-layer controllers, for two tugs. The desired geometry relationship between the ship and tug is used for the computation (as shown in Fig. 4 and Fig. 5).

According to the relationship in Fig. 4, the desired position and heading of Tug 1 can be expressed as:

$$\begin{aligned} \begin{bmatrix} x_{1\mathrm{d}} \\ y_{1d} \\ \psi_{1d} \end{bmatrix} &= \begin{bmatrix} x \\ y \\ \psi \end{bmatrix} + \begin{bmatrix} -\sin(\psi) \\ -\cos(\psi) \\ 0 \end{bmatrix} l_1 + \\ &\begin{bmatrix} -\sin(\psi + \alpha_1) \\ -\cos(\psi + \alpha_1) \\ 0 \end{bmatrix} (l_{\mathrm{tow}_1} + l_{\mathrm{T}_1}) + \begin{bmatrix} 0 \\ 0 \\ 1 \end{bmatrix} \alpha_1, \end{aligned} \tag{10}$$

where l_{tow_1} is the length of the towline 1.

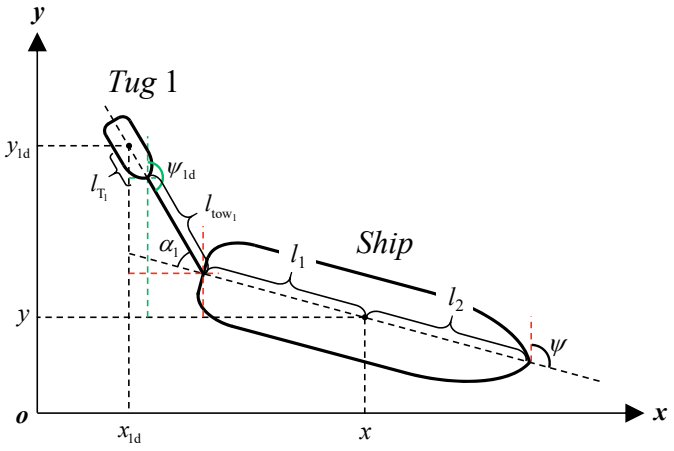

Fig. 4. Geometry diagram of Tug 1 and the Ship.

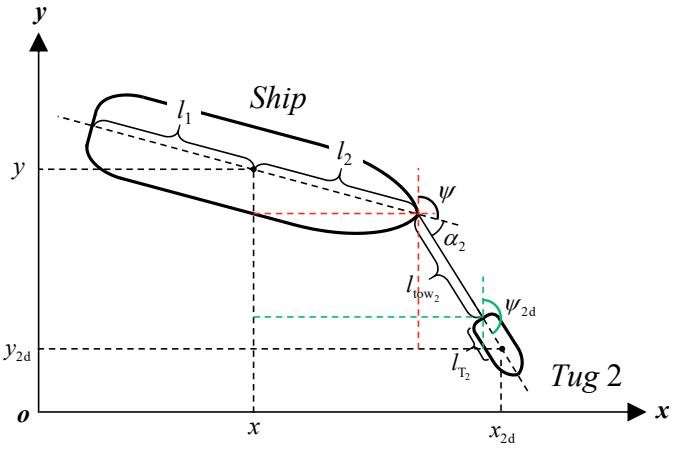

Fig. 5. Geometry diagram of the Tug 2 and the Ship.

According to the relationship in Fig. 5, the desired position and heading of Tug 2 can be expressed as:

$$\begin{bmatrix} x_{2d} \\ y_{2d} \\ \psi_{2d} \end{bmatrix} = \begin{bmatrix} x \\ y \\ \psi \end{bmatrix} + \begin{bmatrix} \sin(\psi) \\ \cos(\psi) \\ 0 \end{bmatrix} l_2 + \begin{bmatrix} \sin(\psi+\alpha_2) \\ \cos(\psi+\alpha_2) \\ 0 \end{bmatrix} (l_{\text{tow}_2} + l_{T_2}) + \begin{bmatrix} 0 \\ 0 \\ 1 \end{bmatrix} \alpha_2, \tag{11}$$

where l_{tow_2} is the length of the towline 2.

It can be seen from (10) and (11) that the reference trajectory of two tugs are related to the position state of the ship ($[x\ y\ \psi]^{\text{T}}$) and the towing angle (α_i). Thus, the desired position vector of the tug can be expressed as:

$$\boldsymbol{\eta_{id}} = \begin{bmatrix} x_{i\text{d}} \\ y_{i\text{d}} \\ \psi_{i\text{d}} \end{bmatrix} = f_i(\boldsymbol{\eta}_{\text{E}}, \alpha_i), \tag{12}$$

where $\boldsymbol{\eta}_{\text{E}}$ is the expected trajectory of the ship calculated from the supervisory controller; f_i stands for (10) (i=1) and (11) (i=2).

3.3 Tug Controller

The objective of the tug controller is to determine the thruster forces and moment ($\boldsymbol{\tau_i}(t)$) for a tug to track the real-time reference trajectories ($\boldsymbol{\eta_{id}}(t)$) . The cost function of this controller is defined for Tug i as:

$$\begin{aligned} J_i(t) &= (\boldsymbol{e_{\eta_i}}(t))^{\text{T}} \boldsymbol{e_{\eta_i}}(t) \\ \boldsymbol{e_{\eta_i}}(t) &= \boldsymbol{\eta_{iC}}(t) - \boldsymbol{\eta_{id}}(t), \end{aligned} \tag{13}$$

where $\boldsymbol{e_{\eta_i}}(t)$ is the position error; $\boldsymbol{\eta_{iC}}(t)$ is the calculated tug position, which satisfies the tug dynamics constraints ((4) and (5)):

$$\begin{aligned} \dot{\boldsymbol{\eta}}_{\boldsymbol{iC}}(t) &= \boldsymbol{R_i}(\psi_{i\text{C}}(t))\boldsymbol{\nu_{iC}}(t) \\ \dot{\boldsymbol{\nu}}_{\boldsymbol{iC}}(t) &= \boldsymbol{M_i}^{-1}[-\boldsymbol{C_i}(\boldsymbol{\nu_{iC}}(t))\boldsymbol{\nu_{iC}}(t) - \boldsymbol{D_i}\boldsymbol{\nu_{iC}}(t) \\ &\quad + \boldsymbol{B_i}(\beta_i(t))F_i(t) + \boldsymbol{\tau_i}(t)], \end{aligned} \tag{14}$$

According to the relationship among tugging angle β_i, desired tug heading $\psi_{i\text{d}}$ and actual tug heading ψ_i (shown in Fig. 6), the tugging angle can be expressed as:

$$\beta_i = \psi_{i\text{d}} - \psi_i, \tag{15}$$

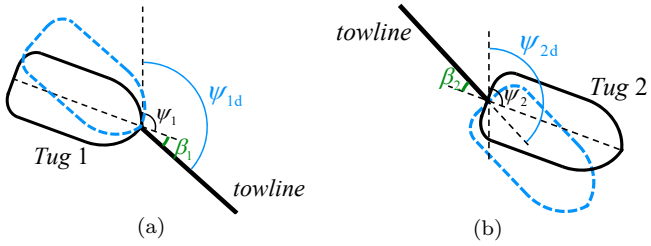

Fig. 6. Relationship among tugging angle β_i, desired tug heading $\psi_{i\text{d}}$ and actual tug heading ψ_i: (a) Tug 1; (b) Tug 2.

In addition, the forces and moment of the thrusters have to satisfy saturation constraints:

$$\boldsymbol{\tau_i} \in [-\boldsymbol{\tau_{i\,\max}}\ ,\ \boldsymbol{\tau_{i\,\max}}] \quad (i = 1, 2) \tag{16}$$

where $\boldsymbol{\tau_{i\,\max}}$ is the maximum value of the thruster forces and moment.

4. SIMULATION RESULTS

In this section, simulation results are presented to show the performance of the proposed control method when applying these to scale ship models.

4.1 Simulation setup

The two tugs are represented by the "*TitoNeri*", which is developed by TU Delft (Haseltalab and Negenborn (2019)). The ship model considered is the "*CyberShip II*", which has been developed by NTNU (Skjetne et al. (2004)).

The parameters of the vessels and towing system are given in Table 1 and 2, respectively. The values of the weight coefficients for the controller are chosen as $w_1 = 1$, $w_2 = 150$, which means that the controller puts more penalties on velocity to make the towing trajectory smoother.

The initial position of the ship is located at the origin with zero degree of heading and no speed. The coordinates of the desired position are $(x_{\text{d}}, y_{\text{d}}) = (40, 25)$, and the desired heading is $\psi_{\text{d}} = 90°$ with no speed.

Table 1. Parameters of "*CyberShip II*" and "*TitoNeri*".

Vessel	Length (m)	Width (m)	Mass (kg)	Actuators
CyberShip II	1.255	0.29	23.8	1. Two stern propellers with two rudders; 2. One bow thruster
TitoNeri	0.97	0.30	16.9	1. Two stern azimuth thrusters; 2. One bow thruster

Table 2. Parameters of the towing system.

Length of towline	$l_{\text{tow}_1} = 1\text{m}$	$l_{\text{tow}_2} = 1\text{m}$
Distance from the ship centers of gravity	$l_1 = 0.67\text{m}$	$l_2 = 0.585\text{m}$
Distance from the tug centers of gravity	$l_{\text{T}_1} = 0.5\text{m}$	$l_{\text{T}_2} = 0.5\text{m}$
Maximum values of the towing forces	$F_{1\,\max} = 3\text{N}$	$F_{2\,\max} = 3\text{N}$
Maximum values of the thruster forces	$\tau_{1\,\max} = 5\text{N}$	$\tau_{2\,\max} = 5\text{N}$
Maximum rate of change of towing angles	$\bar{\alpha}_1 = 5°/\text{s}$	$\bar{\alpha}_2 = 5°/\text{s}$
Maximum rate of change of towing forces	$\bar{F}_1 = 1\text{N/s}$	$\bar{F}_2 = 1\text{N/s}$

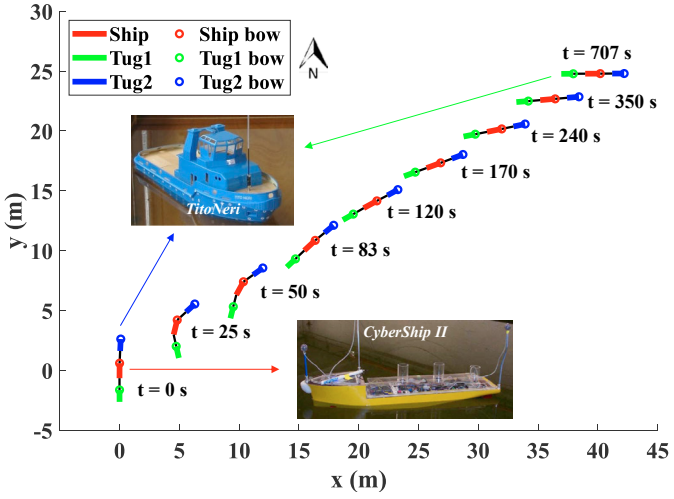

Fig. 7. Simulated towing process.

4.2 Results and discussion

The towing process is shown in Fig. 7, and the time-varying states of the ship are shown in Fig. 8.

As seen in Fig. 7, the ship (red one) is moved from position $(0, 0)$ to position $(40, 25)$ by the two autonomous tugs (the green and blue one), and its heading is changed from 0 to 90 degree during the process. The goal of $\boldsymbol{\eta}_{\mathbf{d}}$ is achieved. It can be also found that for the first 350 s, the towing system has already done most of the route. However, the rest little part of the route also takes about 350 s (from 350 s to 707 s) to achieve the final goal. The reason is that as the ship

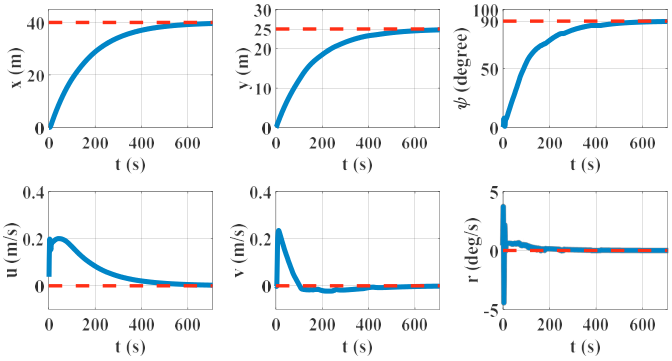

Fig. 8. Position (x, y), heading ψ and velocities (u, v, r) of the ship.

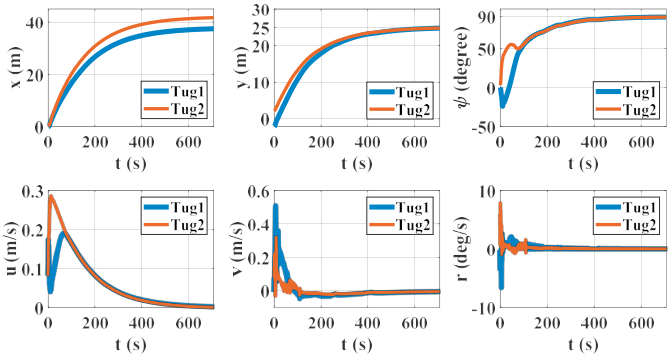

Fig. 9. Time-varying states of two tugs.

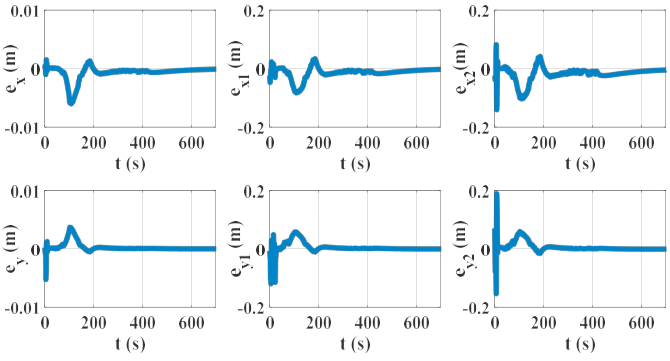

Fig. 10. Position errors of the three vessels.

approaches the goal, its velocity has to be decreased and finally becomes zero. What the controllers do in the rest little part of the route is to regulate the ship velocity. This can be seen in Fig. 8 the time-varying velocities. Thus, the goal of $\boldsymbol{\nu}_{\mathbf{d}}$ is also achieved. In addition, Fig. 9 shows the time-varying states of the two tugs, which reflects that when the ship gradually reaches the goal, the two tugs also converge to the specific states.

The performance of trajectory tracking can be assessed by the position errors $(e_x = x - x_{\text{d}}, e_y = y - y_{\text{d}})$ of the three vessels as shown in Fig. 10. It can be seen that all the errors converge to 0. The maximum position error for the ship is less than 0.01 meters, and for the tugs is less than 0.2 meters. Considering the length of the ship and tugs, this value of maximum errors can be accepted.

5. CONCLUSIONS AND FUTURE RESEARCH

This paper focuses on the cooperative control of autonomous tugs for ship towing in a berthing scenario. We propose a multi-layer control strategy for the towing system to guarantee the ship reaches a desired position with desired heading and velocity. In the supervisory controller, a control method is used to allocate the towing forces and determine the towing angles. By combining the geometry relationships, the reference trajectories of the two autonomous tugs can be calculated online. Based on the reference, the trajectory tracking, which is in the lower layer control, is addressed. Simulation experiments illustrate the performance of the proposed control method. The results indicate that the two autonomous tugs can cooperatively tow an unpowered ship to a desired position with desired heading and velocity.

This paper is a conceptual step toward autonomous tug-assisted motion control using simplified model-scale vessels. Future research will focus on the following issues: 1) actual model tests of the model-scale vessels; 2) robustness of the towing system for the environmental disturbances; 3) collision avoidance of the towing system for the complex traffic environment; 4) uncertainties of the towing system.

ACKNOWLEDGEMENTS

This research is supported by the China Scholarship Council under Grant 201806950080 and the Researchlab Autonomous Shipping (RAS) of Delft University of Technology.

REFERENCES

Bertram, V. (2008). Unmanned surface vehicles-a survey. In *Proceedings of the Skibsteknisk Selskab*, 1–14. Copenhagen, Denmark.

Bhattacharya, S., Heidarsson, H., Sukhatme, G.S., and Kumar, V. (2011). Cooperative control of autonomous surface vehicles for oil skimming and cleanup. In *Proceedings of the 2011 IEEE International Conference on Robotics and Automation*, 2374–2379. Shanghai, China.

Bidikli, B., Tatlicioglu, E., and Zergeroglu, E. (2016). Robust dynamic positioning of surface vessels via multiple unidirectional tugboats. *Ocean Engineering*, 113, 237–245.

Bui, V.P., Ji, S.W., Jang, J.S., and Kim, Y.B. (2012). Ship trajectory tracking in harbour area by using autonomous tugboats. *IFAC Proceedings Volumes*, 45(13), 740–745.

Chen, L., Hopman, H., and Negenborn, R.R. (2018). Distributed model predictive control for vessel train formations of cooperative multi-vessel systems. *Transportation Research Part C: Emerging Technologies*, 92, 101–118.

Devaraju, A., Chen, L., and Negenborn, R.R. (2018). Autonomous surface vessels in ports: Applications, technology and port infrastructures. In *Proceedings of the 9th International Conference on Computational Logistics (ICCL 2018)*, 85–105. Vietri sul Mare, Italy.

Esposito, J., Feemster, M., and Smith, E. (2008). Cooperative manipulation on the water using a swarm of autonomous tugboats. In *Proceedings of the 2008 IEEE International Conference on Robotics and Automation*, 1501–1506. Pasadena, CA, USA.

Fossen, T.I. (2011). *Handbook of Marine Craft Hydrodynamics and Motion Control*. John Wiley & Sons, Chichester, West Sussex, UK.

Giron-Sierra, J.M., Gheorghita, A.T., Angulo, G., and Jimenez, J.F. (2014). Towing a boom with two USVs for oil spill recovery: Scaled experimental development. In *Proceedings of the 13th International Conference on Control Automation Robotics & Vision (ICARCV)*, 1729–1734. Singapore, Singapore.

Hajieghrary, H., Kularatne, D., and Hsieh, M.A. (2017). Cooperative transport of a buoyant load: A differential geometric approach. In *Proceedings of the 2017 IEEE/RSJ International Conference on Intelligent Robots and Systems (IROS)*, 2158–2163. Vancouver, BC, Canada.

Haseltalab, A. and Negenborn, R.R. (2019). Model predictive maneuvering control and energy management for all-electric autonomous ships. *Applied Energy*, 251, 113308.

Hensen, H. (2003). *Tug Use in Port: A Practical Guide*. Nautical Institute, London, UK.

Johansen, T.A. and Fossen, T.I. (2013). Control allocation—a survey. *Automatica*, 49(5), 1087–1103.

Liu, Z., Zhang, Y., Yu, X., and Yuan, C. (2016). Unmanned surface vehicles: An overview of developments and challenges. *Annual Reviews in Control*, 41, 71–93.

Manley, J.E. (2008). Unmanned surface vehicles, 15 years of development. In *Proceedings of the OCEANS 2008*, 1–4. Quebec, Canada.

Pereda, F.J., De Marina, H.G., Giron-Sierra, J.M., and Jimenez, J. (2011). Towards automatic oil spill confinement with autonomous marine surface vehicles. In *Proceedings of the OCEANS 2011*, 1–6. Santander, Spain.

Portmann, H.H., Cooper, S., Norton, M., and Newborn, D. (2002). Unmanned surface vehicles: Past, present, and future. *Unmanned Systems*, 20(5), 32–37.

Roberts, G.N. and Sutton, R. (2006). *Advances in Unmanned Marine Vehicles*, volume 69. IET, London, UK.

Sartoretti, G., Shaw, S., and Hsieh, M.A. (2016). Distributed planar manipulation in fluidic environments. In *Proceedings of the 2016 IEEE International Conference on Robotics and Automation (ICRA)*, 5322–5327. Stockholm, Sweden.

Skjetne, R., Smogeli, Ø., and Fossen, T.I. (2004). Modeling, identification, and adaptive maneuvering of Cybership II: A complete design with experiments. *IFAC Proceedings Volumes*, 37(10), 203–208.

Smith, E.T., Feemster, M.G., and Esposito, J.M. (2007). Swarm manipulation of an unactuated surface vessel. In *Proceedings of the 2007 Thirty-Ninth Southeastern Symposium on System Theory*, 16–20. Macon, GA, USA.

Yan, R., Pang, S., Sun, H., and Pang, Y. (2010). Development and missions of unmanned surface vehicle. *Journal of Marine Science and Application*, 9(4), 451–457.

Yun, L. and Jian, Z. (2018). Design and implementation of cooperative turning control for the towing system of unpowered facilities. *IEEE Access*, 6, 18713–18722.

Zheng, H., Negenborn, R.R., and Lodewijks, G. (2017). Fast ADMM for distributed model predictive control of cooperative waterborne AGVs. *IEEE Transactions on Control Systems Technology*, 25(4), 1406–1413.